

Supplementary Materials for

In vivo multidimensional CRISPR screens identify *Lgals2* as an immunotherapy target in triple-negative breast cancer

Peng Ji *et al.*

Corresponding author: Zhi-Ming Shao, zhi_ming_shao@163.com; Xin Hu, xihu@fudan.edu.cn;
Gen-Hong Di, genhong_di@163.com

Sci. Adv. **8**, eabl8247 (2022)
DOI: 10.1126/sciadv.abl8247

The PDF file includes:

Figs. S1 to S7
Legends for tables S1 to S8

Other Supplementary Material for this manuscript includes the following:

Tables S1 to S8

Figure S1

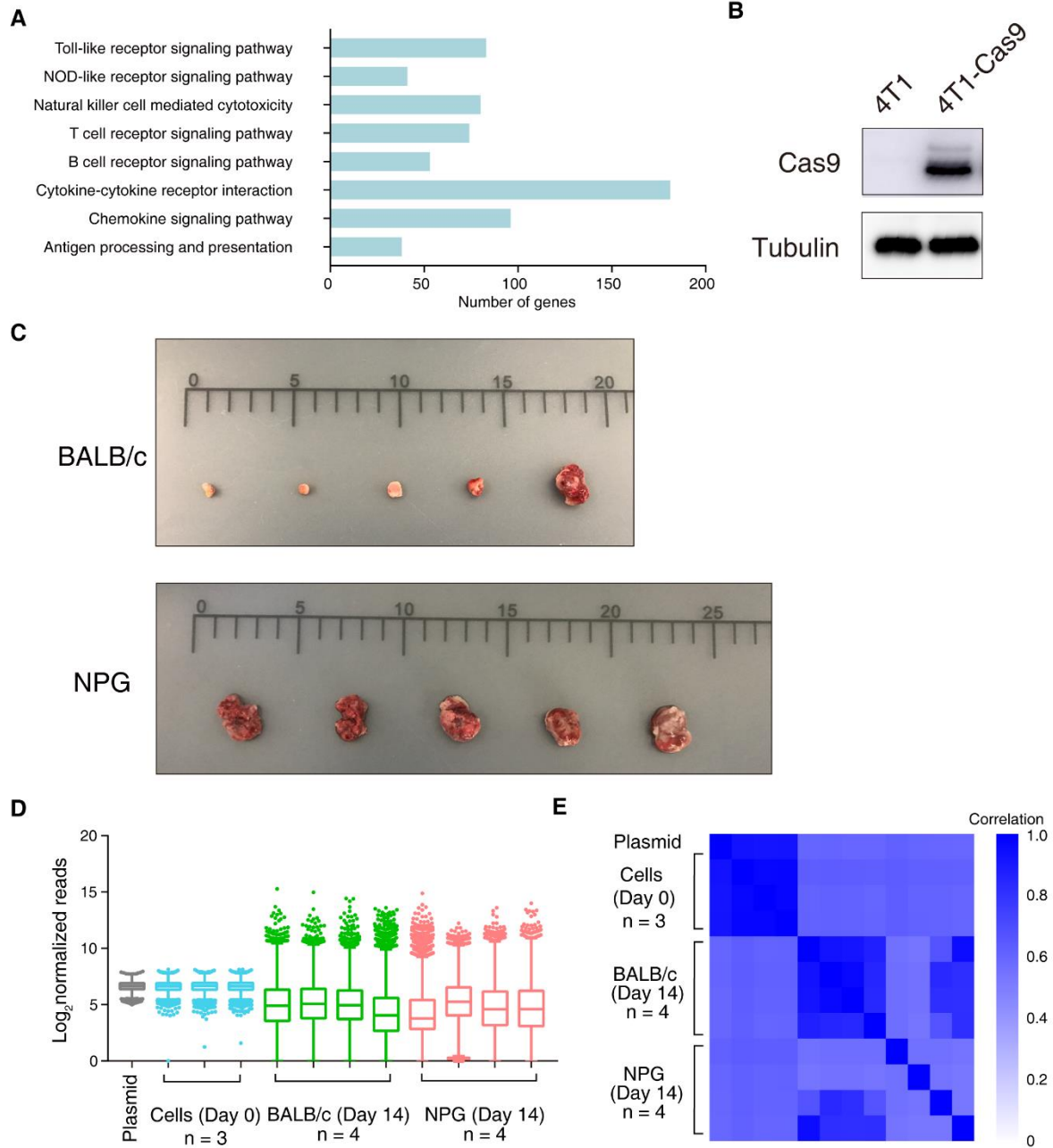


Fig. S1. Analysis of DrIM screen performance.

(A) Histogram showing the number of human disease-related immune genes targeted in the screen in each of the KEGG pathways indicated.

(B) Western blot analysis of 4T1 cell lysate of uninfected cells or after transduction with a lentiviral vector encoding Cas9 for Cas9 and tubulin expression.

(C) *Ex vivo* images of resected tumors from BALB/c mice and NPG mice.

(D) Boxplot of the sgRNA normalized read counts for the DrIM plasmid library, transduced cells before transplantation, tumors in BALB/c mice and tumors in NPG mice. Outliers are shown as colored dots for each respective sample.

(E) Spearman correlation coefficient of the normalized sgRNA read counts from the DrIM plasmid library, transduced cells before transplantation, tumors in BALB/c mice and tumors in NPG mice.

Figure S2

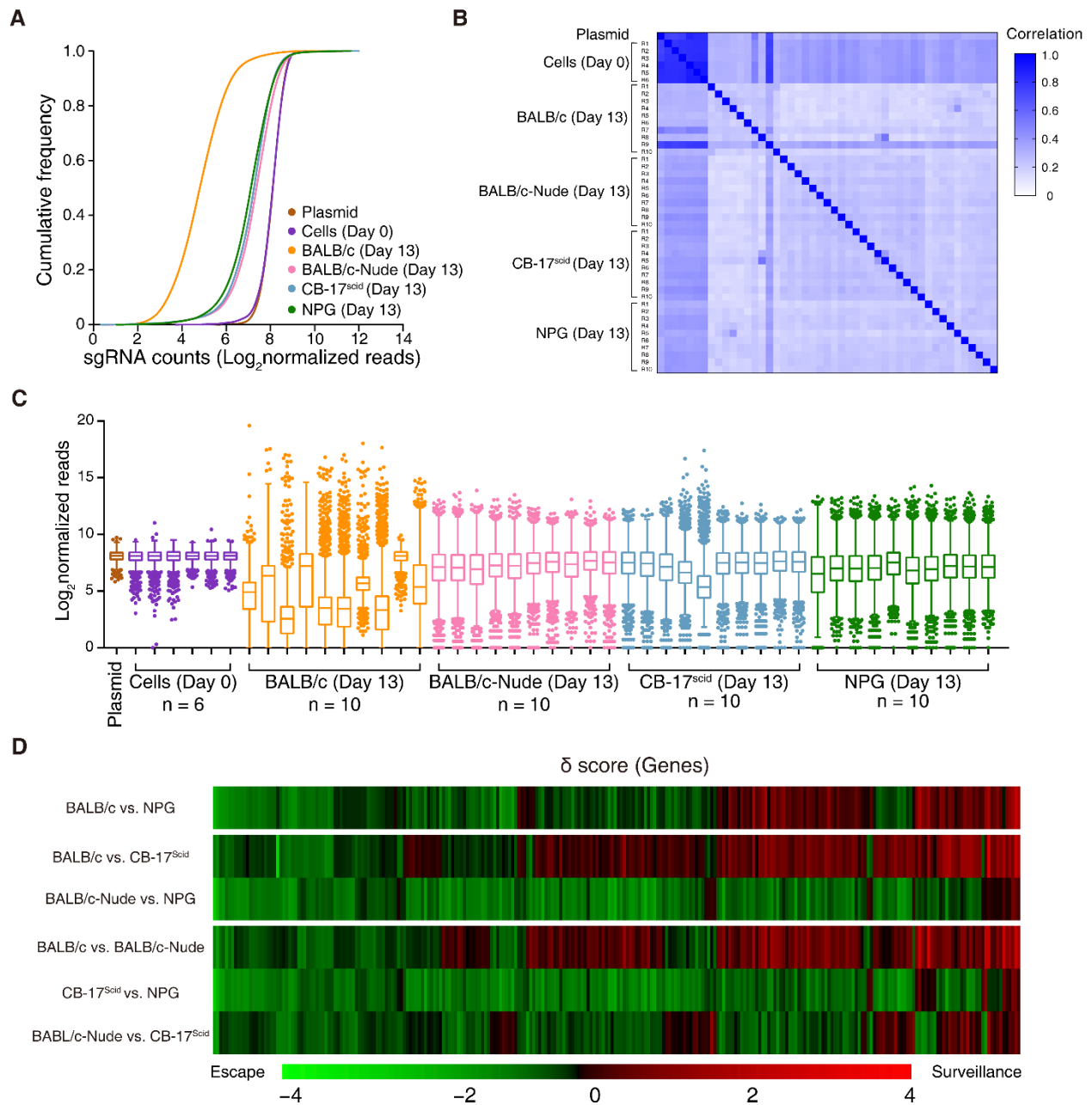


Fig. S2. Analysis of mini-DrIM screen performance.

(A) Cumulative distribution function (CDF) plots of mini-DrIM library sgRNAs in the plasmid, cells before transplantation, tumors in BALB/c mice, tumors in BALB/c-Nude mice, tumors in CB-17^{scid} mice and tumors in NPG mice. Distributions for each sample type are averaged across individual mice and infection replications.

(B) Spearman correlation coefficient of the normalized sgRNA read counts from the mini-DrIM plasmid library, transduced cells before transplantation, tumors in BALB/c mice, tumors in BALB/c-Nude mice, tumors in CB-17^{scid} mice and tumors in NPG mice.

(C) Boxplot of the sgRNA normalized read counts for the mini-DrIM plasmid library, transduced cells before transplantation, tumors in BALB/c mice, tumors in BALB/c-Nude mice, tumors in CB-17^{scid} mice and tumors in NPG mice. Outliers are shown as colored dots for each respective sample.

(D) Heatmap of δ score under different immune-selection pressures.

Figure S3

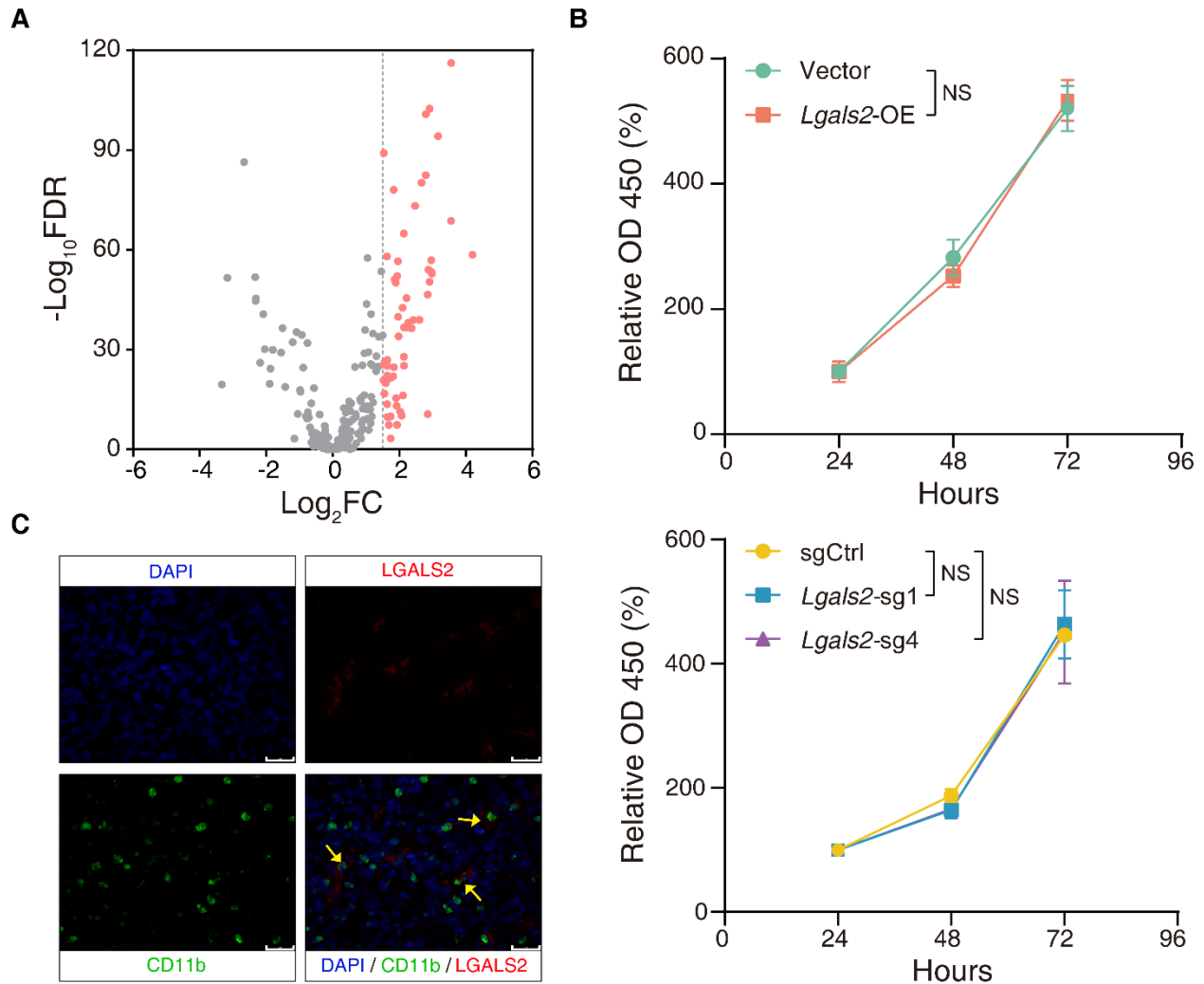


Fig. S3. Identification of putative essential genes mediating immunosuppression in TNBC.

(A) Volcano plot showing comparison of mRNA expression of mini-DrIM library genes between TNBC tumor tissue samples (n = 360) and paired normal samples (n = 88) in the FUSCC cohort.

(B) *In vitro* cell growth curve of 4T1 cells over-expressing *Lgals2* (top panel) or lacking *Lgals2* (bottom panel). NS $P \geq 0.05$. Data are presented as mean \pm s.e.m.

(C) Representative immunofluorescence staining of LGALS2 (red) in combination with CD11b (green) in resected tumors from 4T1 cells transplanted BALB/c mice. Arrows indicate LGALS2 did not express on CD11b⁺ cells. Scale bars, 25 μ m.

Figure S4

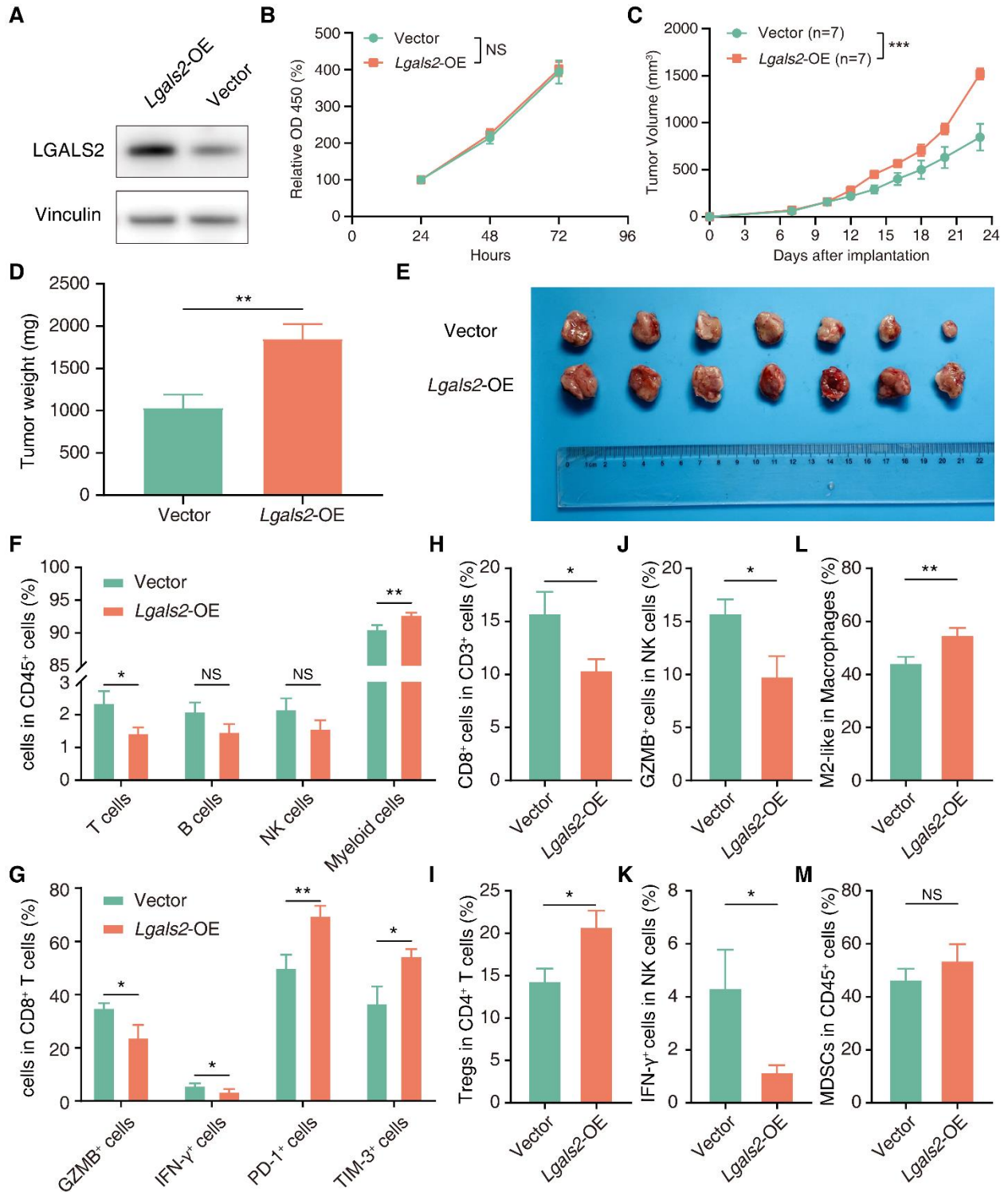


Fig. S4. Identification of *Lgals2* function on EMT6 breast cancer mouse models.

(A) Western blot of *Lgals2* protein level in EMT6 cells transduced with either vector or *Lgals2*-overexpressing plasmid.

(B) *In vitro* cell growth curve of EMT6 cells over-expressing *Lgals2*. NS $P \geq 0.05$. Data are presented as mean \pm s.e.m.

(C-E) *In vivo* analysis of transplanted EMT6 cells with *Lgals2* overexpressing in BALB/c mice including (E) tumor growth curve, (F) tumor weight and (G) *ex vivo* images of resected tumors. *** $P < 0.001$, ** $P < 0.01$. Data are presented as the mean \pm s.e.m.

(F-M) The primary tumors of vector control and *Lgals2*-overexpressing EMT6 tumors of BALB/c mice were harvested for flow cytometry to determine the percentages of (H) T cells, B cells, NK cells and myeloid cells among CD45⁺ cells, (I) Granzyme B⁺ (GZMB⁺) cells, IFN- γ ⁺ cells, PD-1⁺ cells and TIM-3⁺ cells among CD8⁺ T cells, (J) CD8⁺ T cells among CD3⁺ T cells, (K) FOXP3⁺CD25⁺ Tregs among CD4⁺ T cells, (L) GZMB⁺ cells among NK cells, (M) IFN- γ ⁺ cells among NK cells, (N) M2-like macrophages among total macrophages and (O) MDSCs among CD45⁺ cells. ** $P < 0.01$; * $P < 0.05$; NS $P \geq 0.05$. Data are presented as the mean \pm s.e.m.

Figure S5

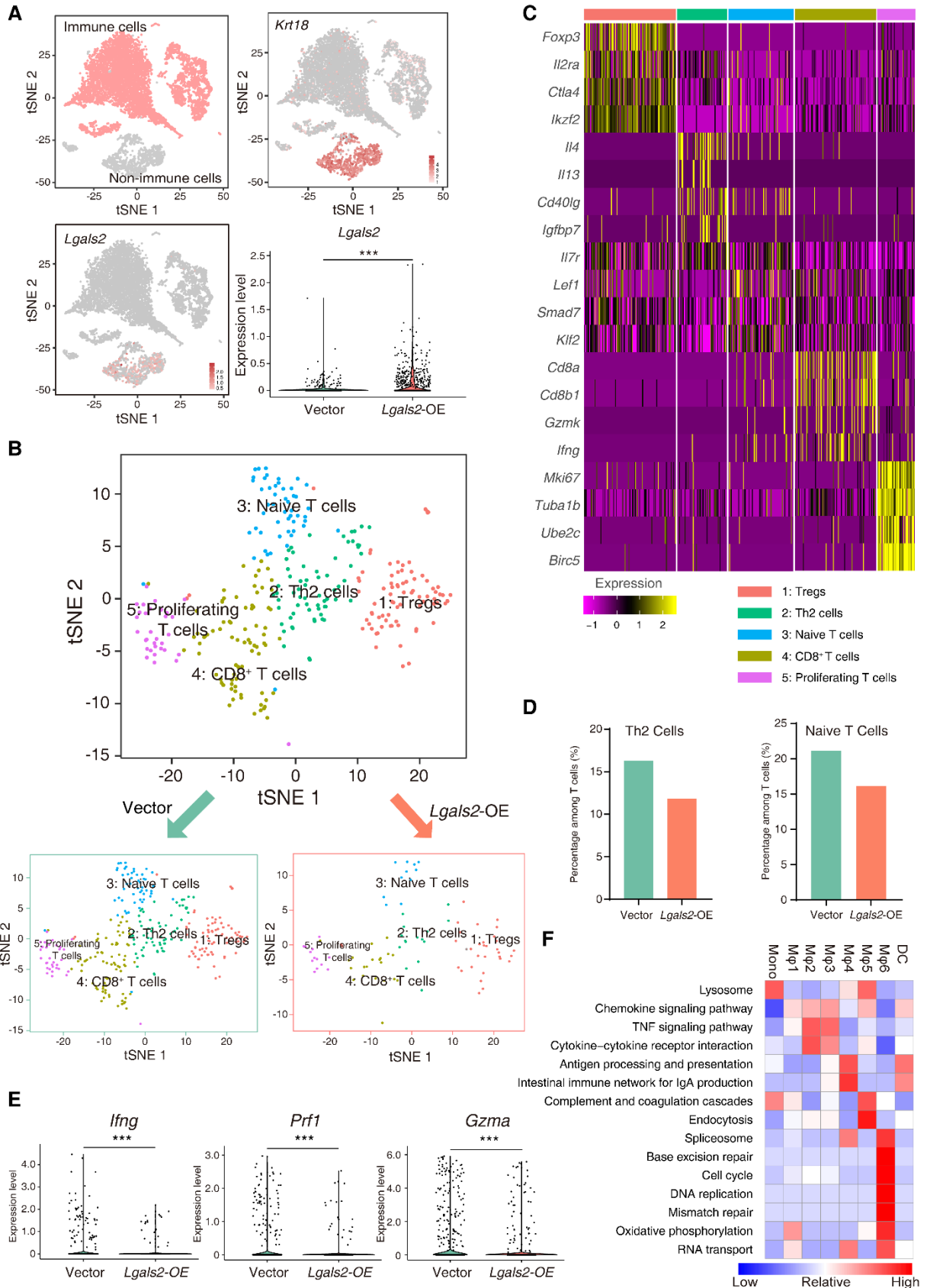


Fig. S5. Single-cell RNA-seq analysis of 4T1 tumors with vector or *Lgals2* overexpression.

(A) t-SNE plot showing identification of immune cells and non-immune cells with marker genes and violin plot of *Lgals2* mRNA levels.

(B) t-SNE plot of re-classification of intratumoral T cells.

(C) Heatmap of key significant genes in clusters of T cells.

(D) The distribution of Th2 and Naïve T cells between Vector and *Lgals2*-OE tumor cells.

(E) Violin plot of *Ifng*, *Prfl* and *Gzma* mRNA levels.

(F) Heatmap of GSEA identifying pathway enrichment by monocytes/dendritic cells/macrophages cluster.

Figure S6

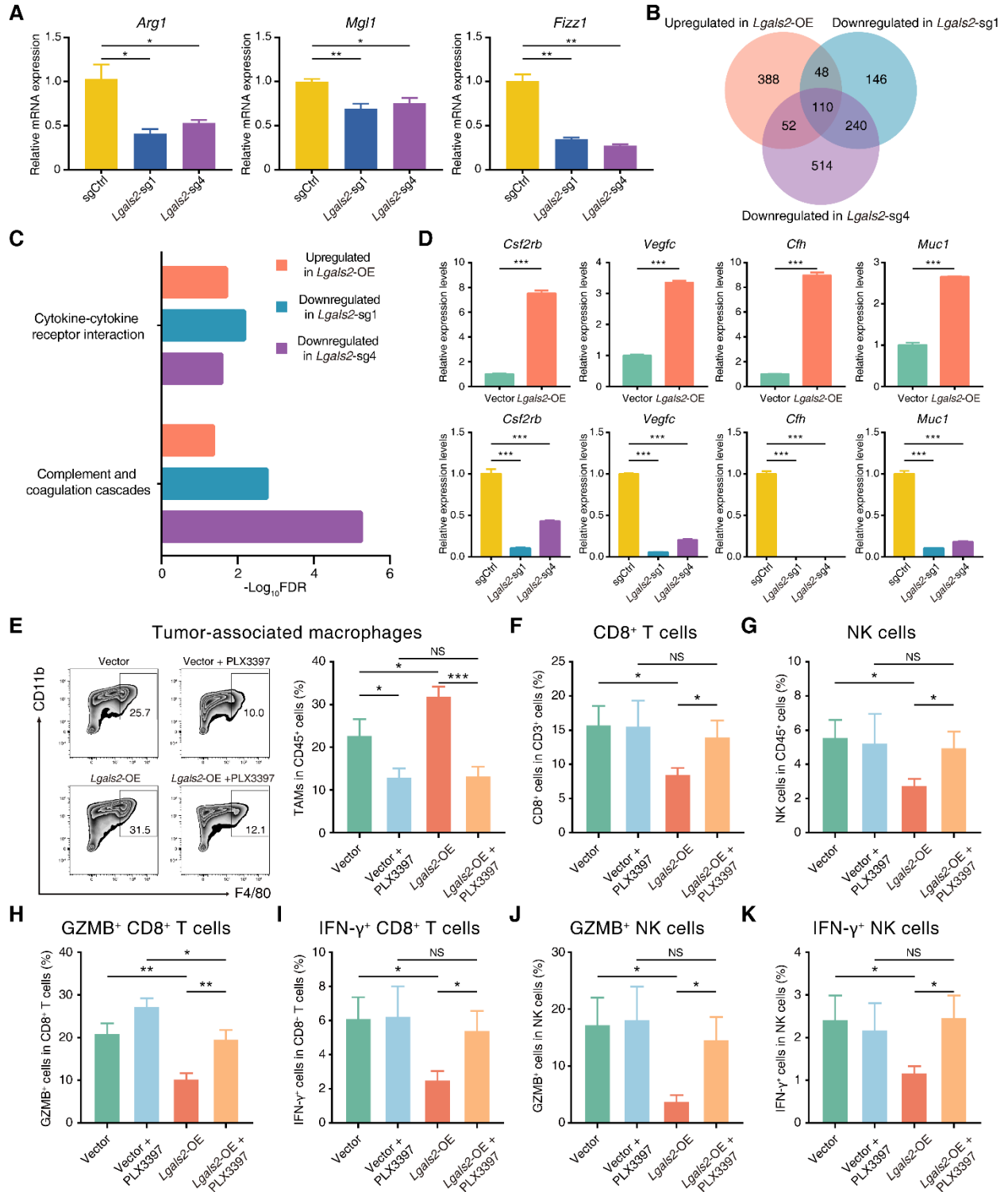


Fig. S6. *Lgals2* facilitates M2-like polarization and proliferation of macrophages through CSF1.

(A) *Arg1*, *Mgl1* and *Fizz1* mRNA in mouse peritoneal macrophages co-cultured with *Lgals2*-knockout and vector control 4T1 cells for 72 hours were analyzed by qPCR. ** $P < 0.01$, * $P < 0.05$. Data are presented as the mean \pm s.e.m.

(B) Venn diagram of significantly upregulated genes in *Lgals2* over-expressing 4T1 tumor cells and significantly downregulated genes in *Lgals2* knockout 4T1 cells *in vitro* from bulk RNA-seq.

(C) GO analysis of significantly upregulated genes in *Lgals2*-overexpressing 4T1 tumor cells and significantly downregulated genes in *Lgals2* knockout 4T1 cells *in vitro* from bulk RNA-seq.

(D) qPCR single-gene validation of representative significantly upregulated or downregulated genes, including *Csf2rb*, *Vegfc*, *Cfh* and *Muc1* in 4T1 cells. *** $P < 0.001$. Data are presented as mean \pm s.e.m.

(E) After study endpoint, the F4/80⁺CD11b⁺ tumor-associated macrophages in 4T1 tumors of BALB/c mice from each group were measured by flow cytometry. Representative plots of individual tumors are shown on the left, and bar graphs of the summary data for all tumors are shown on the right. *** $P < 0.001$; * $P < 0.05$. Data are presented as the mean \pm s.e.m.

(F-K) The primary tumors of 4T1 models from each group were harvested for flow cytometry to determine the percentages of (F) CD8⁺ T cells among CD3⁺ T cells, (G) NK cells among CD45⁺ cells, (H) Granzyme B⁺ (GZMB⁺) cells among CD8⁺ T cells, (I) IFN- γ ⁺ cells among CD8⁺ T cells, (J) GZMB⁺ cells among NK cells and (K) IFN- γ ⁺ cells among NK cells. ** $P < 0.01$; * $P < 0.05$; NS $P \geq 0.05$. Data are presented as the mean \pm s.e.m.

Figure S7

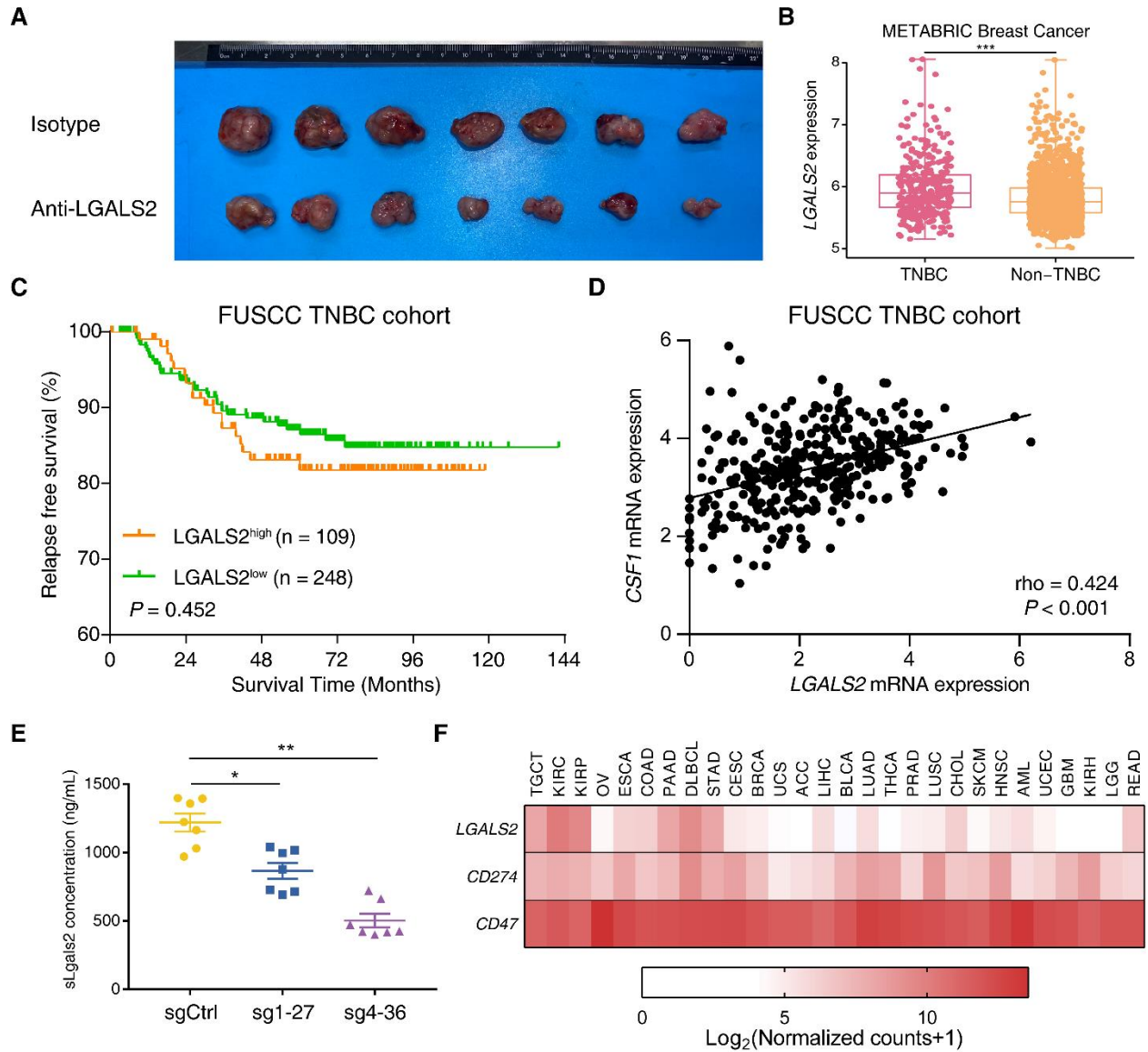


Fig. S7. Blockade of LGALS2 enhances antitumor immune response and shows immunotherapeutic potential of LGALS2 as a target in TNBC cohorts.

(A) Ex vivo images of resected 4T1 tumors receiving isotype or anti-LGALS2 antibody treatment from BALB/c mice.

(B) Box plot showing *LGALS2* mRNA expression level across TNBC and non-TNBC samples in the METABRIC cohort. Whiskers indicate the minimum and maximum values. *** $P < 0.001$.

(C) Kaplan-Meier curves of relapse-free survival between high and low IHC score of LGALS2 for TNBC in the FUSCC cohort.

(D) The association between *LGALS2* and *CSF1* mRNA expression levels in TNBC patient samples from FUSCC (n = 360).

(E) Comparison of serum LGALS2 concentration in the 4T1 transplanted BALB/c mice with either vector control or Lgals2-targeting sgRNAs. * $P < 0.05$, ** $P < 0.01$.

(F) Heat map of expression ($\log_2[\text{normalized counts} + 1]$) of *LGALS2* from bulk TCGA and TARGET studies, as compared to known immune checkpoint molecules *CD274* and *CD47*.

Table S1 (separate file). DrIM sgRNA library annotation.

Table S2 (separate file). δ scores of genes in DrIM sgRNA library.

Table S3 (separate file). Mini-DrIM sgRNA library annotation.

Table S4 (separate file). δ scores of different immune-selection pressures in mini-DrIM sgRNA library.

Table S5 (separate file). Eleven candidate genes related to tumor immune escape in TNBC.

Table S6 (separate file). Correlation between clinicopathologic variables and expression of LGALS2 in 357 cases of TNBC.

Table S7 (separate file). Abbreviations, full names, and number of tumor and healthy samples for TCGA, TARGET, and GTEX studies analyzed in this study.

Table S8 (separate file). Primers and sequences for qPCR.